

Cerebellar and Prefrontal Cortical Alterations in PTSD: Structural and Functional Evidence

Sophie E. Holmes¹, Dustin Scheinost^{2,3}, Nicole DellaGioia¹, Margaret T. Davis², David Matuskey^{1,2}, Robert H. Pietrzak^{1,4}, Michelle Hampson^{1,2,3}, John H. Krystal^{1,4}, and Irina Esterlis^{1,4}

Abstract

Background: Neuroimaging studies have revealed that disturbances in network organization of key brain regions may underlie cognitive and emotional dysfunction in posttraumatic stress disorder (PTSD). Examining both brain structure and function in the same population may further our understanding of network alterations in PTSD.

Methods: We used tensor-based morphometry and intrinsic connectivity distribution to identify regions of altered volume and functional connectivity in unmedicated individuals with PTSD ($n = 21$) and healthy comparison participants ($n = 18$). These regions were then used as seeds for follow-up anatomical covariance and functional connectivity analyses.

Results: Smaller volume in the cerebellum and weaker structural covariance between the cerebellum seed and the middle temporal gyrus were observed in the PTSD group. Individuals with PTSD also exhibited lower whole-brain connectivity in the cerebellum, dorsolateral prefrontal cortex (dlPFC) and medial prefrontal cortex. Functional connectivity in the cerebellum and grey matter volume in the dlPFC were negatively correlated with PTSD severity as measured by the DSM-5 PTSD Checklist (PCL-5; $r = -0.77$, $r = -0.79$). Finally, seed connectivity revealed weaker connectivity within nodes of the central executive network (right and left dlPFC), and between nodes of the default mode network (medial prefrontal cortex and cerebellum) and the supramarginal gyrus, in the PTSD group.

Conclusion: We demonstrate structural and functional alterations in PTSD converging on the PFC and cerebellum. Whilst PFC alterations are relatively well established in PTSD, the cerebellum has not generally been considered a key region in PTSD. Our findings add to a growing evidence base implicating cerebellar involvement in the pathophysiology of PTSD.

Keywords

posttraumatic stress disorder, connectivity, cerebellum, structural, multimodal

Received 30 May 2018; Accepted 11 June 2018

Introduction

Functional and anatomical neuroimaging studies suggest that the symptoms of posttraumatic stress disorder (PTSD) are subserved by alterations in the prefrontal cortex (PFC), amygdala, hippocampus and insula.^{1,2} However, given that brain function arises from integration of information from interconnected networks, the current generation of research has started to focus on the covarying patterns between these regions. A growing number of sophisticated neuroimaging techniques allow for identification of network-level changes in the brain, including functional connectivity where functional magnetic resonance imaging is used to measure correlations

¹Department of Psychiatry, Yale School of Medicine, New Haven, CT, USA

²Radiology and Biomedical Imaging, Yale School of Medicine, New Haven, CT, USA

³Child Study Center, Yale School of Medicine, New Haven, CT, USA

⁴U.S. Department of Veteran Affairs National Center for Posttraumatic Stress Disorder, Clinical Neurosciences Division, VA Connecticut Healthcare System, West Haven, CT, USA

Corresponding author:

Sophie E. Holmes, Yale Translational Brain Imaging Program, Suite 314, 2 Church Street South, New Haven, CT 06519, USA.
Email: sophie.holmes@yale.edu



between spatially distinct regions over time,³ and anatomical covariance, where covariance of brain morphometry can be used to determine putative anatomical networks.⁴ Identifying both the functional and structural changes associated with PTSD at a network level will enhance our understanding of the psychopathology of this disorder and could pave the way for more targeted treatment strategies.

Indeed, network level studies are beginning to characterize altered connectivity in PTSD. Functional connectivity studies have revealed disturbances in large-scale networks including the default mode network (DMN),^{5–8} the salience network^{8–10} and the central executive network (CEN),^{9,11,12} as well as altered relationships between PFC and subcortical regions.^{13–15} However, no known study has evaluated differences in anatomical covariance networks in individuals with PTSD. To date, most connectivity studies in PTSD relied on a priori information to define a seed or network of interest. In contrast, data-driven methods – not constrained to a particular seed or network – allow the detection of alterations across the whole brain. While these methods are now beginning to be used in understanding brain patterns in PTSD,^{16,17} such approaches can be taken one step further by using whole-brain analyses to identify seeds for follow-up network analysis in a data-driven manner. This would allow for detection of connectivity alterations in regions that might otherwise be overlooked using conventional seeds chosen a priori.

We used tensor-based morphometry (TBM) (Hua et al., 2008)¹⁸ and intrinsic connectivity distribution (ICD)¹⁹ to characterize whole-brain structural and functional alterations, respectively. We then used regions of altered volume and functional connectivity as seeds for follow-up anatomical covariance and functional connectivity analyses. We recently applied these methods to an independent cohort of unmedicated patients with major depressive disorder (MDD), which allowed for the joint discovery of alterations in both structural and functional networks associated with MDD.²⁰ Based on existing literature, and the whole-brain approach of the study, we hypothesized that individuals with PTSD would show functional and anatomical alterations within core nodes of networks spanning the entire brain, including default mode, central executive and salience networks.

Methods

Participants

Twenty-one medication-free individuals with PTSD (mean \pm SD age = 35.8 \pm 8.5 years; 11 females) and 18 healthy comparison (HC) individuals (mean \pm SD age = 35.2 \pm 13.3 years; 5 females) participated in the study. Sixteen of the 21 PTSD individuals also met

criteria for MDD but no other comorbid disorders. Diagnoses were confirmed using the Structured Clinical Interview for *Diagnostic and Statistical Manual for Mental Disorders, 5th edition* (DSM-5).²⁰ PTSD and mood symptoms were additionally assessed using the DSM-5 version of the PTSD Checklist (PCL-5),²¹ Montgomery-Åsberg Depression Scale (MADRS),²² Hamilton Depression Rating Scale (HAM-D)^{23,24} and Beck Depression Inventory (BDI).²⁵ Types of trauma in the PTSD group included sexual abuse ($n=8$), military combat ($n=5$), sexual assault ($n=1$), physical abuse ($n=2$), human trafficking ($n=1$), car accident ($n=1$), robbery at gunpoint ($n=1$), witnessing of shooting ($n=1$) and witnessing of stabbing ($n=1$). Participants were recruited through placement of advertisements in the Community and through referrals from the West Haven Veterans Healthcare System. PTSD and HC groups did not differ significantly in terms of age, sex, smoking status or handedness (Table 1).

Participants underwent physical and neurological examination to rule out any major medical or neurological illness, and for women, plasma pregnancy tests. Exclusion criteria were lifetime history of comorbid DSM-5 disorder (with the exception of MDD); alcohol and drug use disorder, except for nicotine dependence; positive urine toxicology or pregnancy tests prior to any scan; psychotropic medication within the past two months; history of loss of consciousness for more than 5 min; significant medical condition and contraindications to MRI scanning. Exclusion criteria were the same for the HC group except for the addition of no current or history of any DSM-5 diagnosis except for

Table 1. Participant characteristics.

Variable	PTSD group ($n=21$)	HC group ($n=18$)	p
Sex (male:female)	9:11	12:6	0.18 ^a
Age (years)	35.8 (8.5)	35.2 (13.3)	0.87 ^b
No. of smokers	5	4	0.81 ^a
Age at onset (years)	17.0 (8.2)	–	–
Duration of illness (years)	17.8 (10.0)	–	–
PCL-5	48.8 (9.8)	–	–
MADRS	19.0 (7.0)	–	–
HAM-D	13.3 (5.5)	–	–
BDI	22.6 (10.4)	–	–

Note: Values are presented as mean (SD). PTSD: posttraumatic stress disorder; HC: healthy comparison; PCL-5: DSM-5 version of the PTSD Checklist; MADRS: Montgomery-Åsberg Depression Scale; HAM-D: Hamilton Depression Rating Scale; BDI: Beck Depression Inventory.

^a p value obtained from chi-square test.

^b p value obtained from independent-samples t test.

nicotine dependence. The study was approved by the Yale University Human Investigation Committee. All participants provided written informed consent prior to participating in the study.

Imaging Parameters

Participants were scanned on a Siemens 3T Tim Trio scanner, later upgraded to a Siemens 3T Prisma scanner (Siemens Medical Systems, Erlangen, Germany). After a localizing scan, a high-resolution 3D volume was collected using a magnetization prepared rapid gradient echo sequence (176 contiguous sagittal slices, slice thickness 1 mm, matrix size 192×192 , field of view = 256 mm, repetition time = 2530 ms, echo time = 2.77 ms, flip angle = 7°). Participants had two 5-min and 40-s functional scans in which they were asked to fixate on a crosshair and remain still and awake. Functional scans consisted of 340 whole-brain volumes acquired using a multiband echo-planar imaging sequence with the following parameters: repetition time = 1000 ms, echo time = 29.6 ms, flip angle = 60° , acquisition matrix = 110×110 , in-plane resolution = 2 mm^2 , 60 axial-oblique slices parallel to the AC-PC line, slice thickness = 2 mm, multiband = 4 and acceleration factor = 2. The scanner upgrade occurred in the middle of the study, with no between-group difference in the proportion of subjects scanned before/after the upgrade ($p = 0.57$).

Tensor-Based Morphometry

Images were skull stripped using FMRIB Software Library (<https://fsl.fmrib.ox.ac.uk/fsl/>). Any remaining nonbrain tissue on MRI was manually removed. All further analyses were performed using BioImage Suite²⁶ unless otherwise specified. Images were aligned to Montreal Neurological Institute (MNI) space using a 12-parameter affine registration by maximizing the normalized mutual information between individual scans and the MNI template brain. These aligned images were averaged together to form the initial template using a non-linear registration. For TBM analysis, all images were non-linearly registered to an evolving group average template in an iterative fashion using a previously validated algorithm.²⁷ The algorithm iterates between estimating a local transformation to align individual brains to a group average template and creating a new group average template based on the previous transformations. The local transformation was modelled using a free-form deformation parameterized by cubic B-splines. This transformation deforms an object by manipulating an underlying mesh of control points. The deformation for voxels in between control points was interpolated using B-splines to form a continuous deformation field. Positions of control points were

optimized using conjugate gradient descent to maximize the normalized mutual information between the template and the individual brains. After each iteration, the quality of the local transformation was improved by increasing the number of control points and decreasing the spacing between control points to capture a more precise alignment. A total of four iterations were performed with decreasing control point spacings of 15 mm, 10 mm, 5 mm and 2.5 mm. To help prevent local minima during optimization, a multi-resolution approach was used and three resolution levels were used at each iteration. The determinant of the Jacobian of the deformation field was used to quantify local volume differences between the registered images and the template. This metric provided an estimate of voxel-wise volume changes for all transformed images with respect to the group averaged template and was used for further analysis.

Seed-Based Anatomical Covariance

All regions of significant volume differences were chosen for (post hoc) anatomical covariance analysis. The volumes of these seed regions, calculated as the average determinant of the Jacobian in the seed, were extracted and used as covariates in linear models (described below).

Functional Connectivity Preprocessing

The first 10 volumes of each functional run were discarded to allow for the magnetization to reach a steady state. Motion correction was performed using SPM8 (<http://www.fil.ion.ucl.ac.uk/spm/>). Images were warped into common space using the non-linear transformation described above using cubic interpolation. Images were iteratively smoothed until the smoothness of any image had a full-width half maximum of approximately 5 mm using AFNI's 3dBlurToFWHM (<http://afni.nimh.nih.gov/afni/>). This iterative smoothing reduces motion-related confounds.²⁸ All further analyses were performed using BioImage Suite.²⁶ Several covariates of no interest were regressed from the data including linear and quadratic drifts, mean cerebral spinal fluid signal, mean white-matter signal and mean grey matter signal. For additional control of possible motion related confounds, a 24-parameter motion model (including six rigid body motion parameters, six temporal derivatives and these terms squared) was regressed from the data. The data were temporally smoothed with a Gaussian filter (approximate cut-off frequency = 0.12 Hz). A canonical grey matter mask defined in common space was applied to the data, so only voxels in the grey matter were used in further calculations. Finally, for each participant, all preprocessed resting-state runs were variance normalized and concatenated.

Motion Analysis

As group differences in motion have been shown to confound connectivity studies, we calculated the average frame-to-frame displacement for each participant's data. In line with current reports, participants with an average frame-to-frame displacement greater than 0.20 mm for any run were removed from the analysis (one HC was removed based on this threshold before further analysis). There were no significant differences for motion between the PTSD and the HC groups (MDD: 0.086 ± 0.04 mm, HC: 0.076 ± 0.02 mm, $p = 0.33$). Finally, we regressed a 24-parameter motion model and used an iterative smoothing algorithm to minimize any motion confounds.²⁸

Intrinsic Functional Connectivity

After preprocessing, functional connectivity of each voxel, as measured by ICD, was calculated for each subject as described previously.¹⁸ Similar to other data-driven, voxel-based measures,^{16,29} ICD involves correlating the time series for any voxel with every other time series in the brain or brain hemisphere and then calculating a summary statistic based on the network theory measure *degree*. ICD avoids the need for choosing an arbitrary connectivity threshold by modelling the entire distribution of correlation thresholds using a Weibull distribution: $\frac{\beta}{\alpha} \left(\frac{r}{\alpha}\right)^{\beta-1} \exp\left(-\left(\frac{r}{\alpha}\right)^\beta\right)$, where r is a correlation between two time series, α is the variance parameter and β is the shape parameter. This parameterization is akin to modelling the change in network theory metric *degree*, as the threshold used to calculate *degree* is increased, with a stretched exponential: $\exp\left(-\frac{r^\beta}{\alpha}\right)$, where τ is the correlation threshold, and α and β are the parameters as above.

Specifically, the time series for any grey matter voxel was correlated with every other voxel in the grey matter. A histogram of these correlations was constructed to estimate the distribution of connections to the current voxel. This distribution was converted to a survival function, and the survival function was fitted with a stretched exponential with unknown variance. As variance controls the spread of the distribution of connections, a larger variance indicates a greater number of high correlation connections. Finally, this process is repeated for all voxels in the grey matter resulting in a whole-brain parametric image summarizing the connectivity of each tissue element.

Follow-Up Seed Connectivity

Follow-up seed analysis was performed to explore (post hoc) the nodes identified by ICD analysis to determine the specific connections that were most

responsible for changes in connectivity. The time series of each voxel of the seed region was averaged for each participant. This time series was correlated with the time series for every other voxel in the grey matter to create a map of r values, reflecting seed-to-whole-brain connectivity. These r values were then transformed to z values using Fisher's transform yielding one map for each participant representing the strength of correlation to the seed region.

Group Analysis

Primary analyses included TBM and ICD group differences between the HC and the PTSD groups, and voxel-wise correlations between TBM and ICD values and PCL-5 scores. These analyses were corrected for multiple comparisons at the experiment level, such that findings from the four primary analyses were considered significant at a Bonferroni corrected threshold of $p < 0.0125$ ($p < 0.05$ divided by four analyses). Exploratory analyses included correlations with sub-scales of the PCL-5, mood rating scales (MADRS, HAM-D and BDI), and follow-up seed covariance and connectivity. TBM and seed anatomical covariance data were analyzed with voxel-wise general linear modelling. For primary analyses and seed region analyses, the regressor of interest was group (for the group contrasts) or PCL score (for symptom correlations). Correlations with symptoms were restricted to the PTSD group. Age at scan and sex were included as covariates. For models of anatomical covariance, seed volume was also included as a covariate of interest, and the group-by-volume interaction was examined. Regions showing significant group-by-volume interaction are regions where the correlation between the volume of that region and the seed region is different between groups. Voxel-wise t tests were used to compare the connectivity data between the study groups. Functional (ICD and seed) and structural (TBM and seed) imaging results are shown at a cluster-level threshold of $p < 0.0125$ (for primary analyses) or $p < 0.05$ (for exploratory analyses) with family-wise error correction as determined by AFNI's 3dClustSim program (version 16.0.09) using a cluster-forming threshold of $p = 0.005$, 10,000 iterations, a grey matter mask and a smoothness estimated from the residuals using 3dFWHMx.

Results

Primary Results

TBM. TBM analysis revealed significantly smaller volume in the right cerebellar crus in the PTSD compared to HC group ($p < 0.0125$, corrected) (Figure 1(a)). No regions of greater volume for the PTSD versus HC groups were detected. Voxel-wise correlations between TBM values

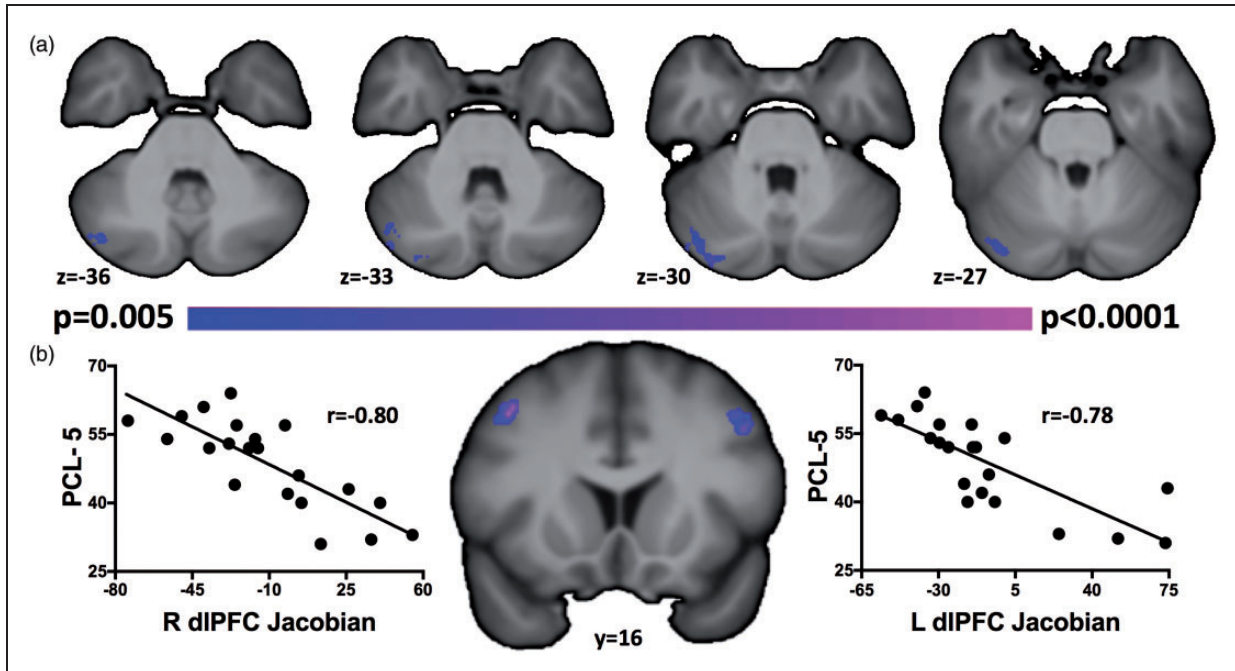


Figure 1. TBM analysis. (a) Transverse images displaying lower cerebellar volume in PTSD versus HC groups ($p < 0.0125$, corrected). (b) Voxel-wise negative correlations between TBM values in dIPFC and PCL scores ($p < 0.0125$, corrected). dIPFC: dorsolateral prefrontal cortex; PCL-5: DSM-5 version of the PTSD Checklist.

and PCL scores revealed significant negative correlation in the right ($r = -0.80$) and left ($r = -0.78$) posterior dorsolateral PFC ($p < 0.0125$, corrected) (Figure 1(b)).

ICD Functional Connectivity. Compared to the HC group, the PTSD group displayed significantly lower ICD connectivity in the right and left dIPFC, left medial prefrontal cortex (mPFC) and the right cerebellar crus ($p < 0.0125$, corrected) (Figure 2(a)). No regions of greater connectivity for the PTSD versus HC groups were detected. Voxel-wise correlation between ICD connectivity and PCL scores revealed a significant negative correlation in the cerebellar vermis ($r = -0.77$, $p < 0.0125$, corrected) (Figure 2(b)).

Using extracted TBM and ICD values from the significant clusters, we performed between-group comparisons and correlations with symptoms while controlling for scanner type and sex (included as covariates). The significant findings remained unchanged. Between-group results remained significant when examining data from subjects scanned on the Trio and Prisma independently. Furthermore, structural and functional findings did not differ between PTSD individuals with and without MDD, and there were no main effects of sex.

Secondary Results

Associations With Other Symptoms. In an exploratory manner, TBM and ICD values were extracted from

each cluster of group differences and used for correlation with mood symptoms (MADRS, BDI and HAM-D). No significant correlations were observed for mood symptoms or for duration of illness (all p values > 0.20). TBM and ICD values were extracted from each cluster of correlation with the PCL and used for correlation with PCL sub-scales. ICD values in the cerebellum were negatively correlated with all symptom cluster scores (intrusion symptoms ($r = -0.62$, $p = 0.003$), avoidance ($r = -0.45$, $p = 0.04$), negative alterations in mood and cognition ($r = -0.75$, $p < 0.0001$) and alterations in arousal and reactivity ($r = -0.75$, $p = 0.0001$) (Figure S1(a)). TBM values in right and left dIPFC were negatively correlated with all symptom cluster scores, with the exception of PCL-5 avoidance scores (all r values < -0.65 , all p values < 0.0003) (Figure S1(a) and (b)).

Anatomical Covariance. The cerebellar cluster identified in the TBM analysis (Figure 1) was used as a seed for anatomical covariance analysis to identify any network-level structural differences between PTSD and HC groups. Using the cerebellum cluster as seed, the PTSD group exhibited significantly lower covariance with the superior temporal sulcus/middle temporal gyrus compared to the HC group ($p < 0.05$, corrected; Figure 3(a)). The HC group showed a significant positive correlation between the two regions ($r = 0.69$, $p = 0.001$) while the PTSD group did not ($r = -0.14$, $p = 0.55$) (Figure 3(b)).

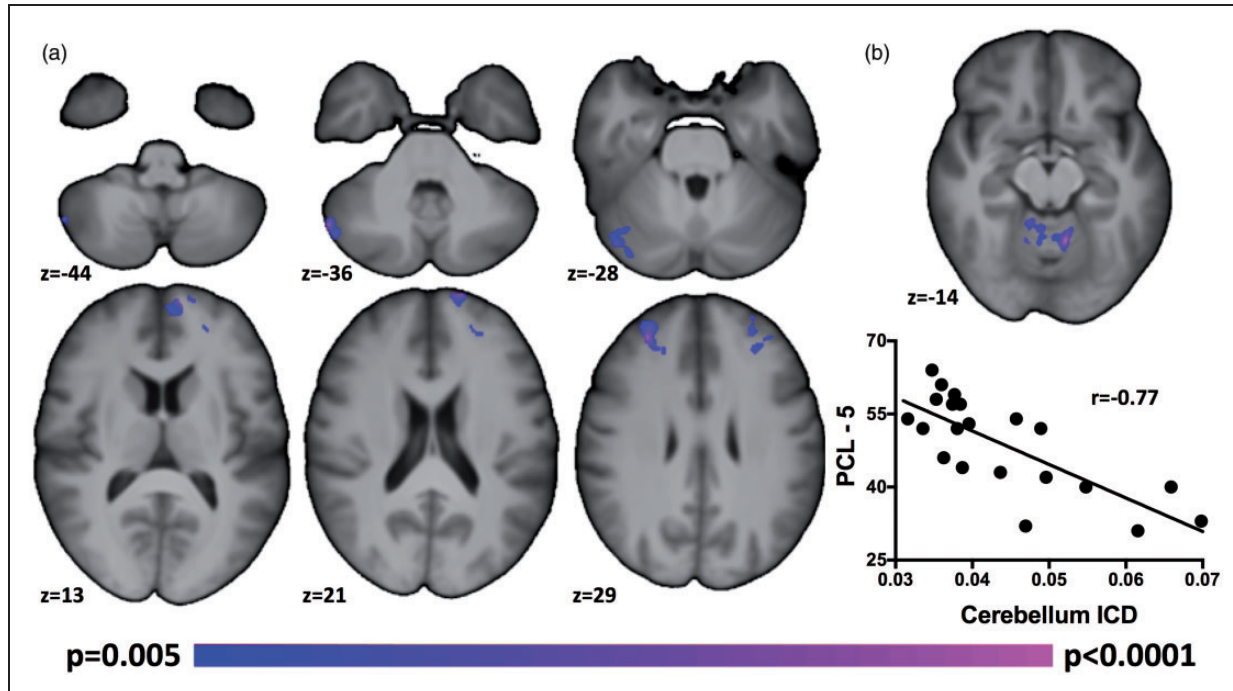


Figure 2. ICD functional connectivity. (a) Transverse images displaying lower ICD functional connectivity in cerebellum, mPFC and dIPFC in PTSD versus HC groups ($p < 0.0125$, corrected). (b) Voxel-wise negative correlation between ICD connectivity in the cerebellum and PCL scores ($p < 0.0125$, corrected).

ICD: intrinsic connectivity distribution; PCL-5: DSM-5 version of the PTSD Checklist.

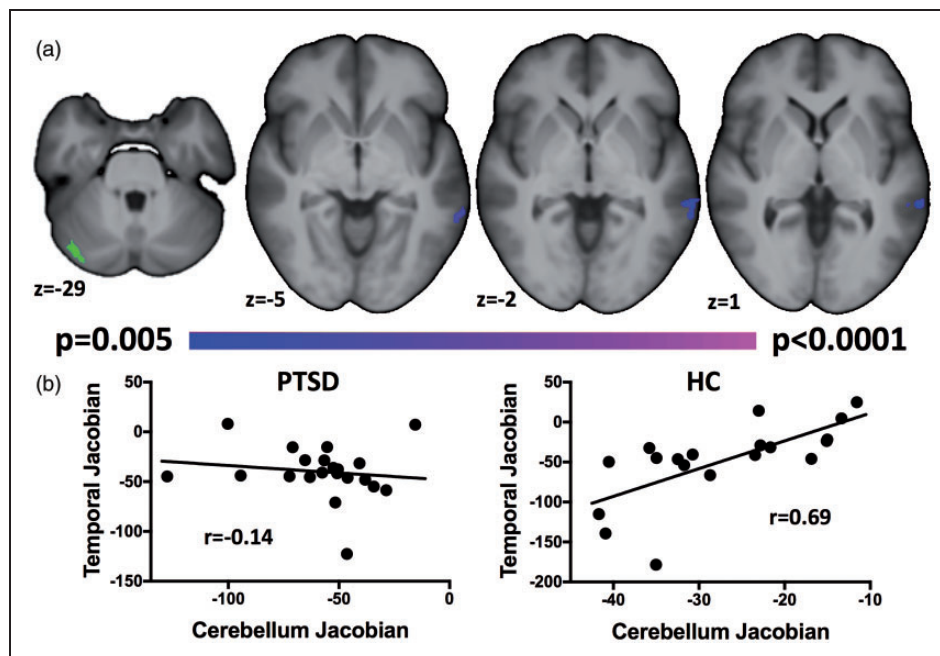


Figure 3. Anatomical covariance. (a) Transverse images displaying decreased anatomical covariance between the cerebellar seed (left, green) and the middle temporal gyrus ($p < 0.05$, corrected). (b) Positive and negative correlations between the two regions in PTSD, respectively (left) and HC (right).

PTSD: posttraumatic stress disorder.

Seed-Based Connectivity. The dlPFC, mPFC and cerebellum regions were used in follow-up seed connectivity analysis. In the PTSD group, the cerebellum and mPFC seeds showed significantly stronger connectivity (reduced negative connectivity) to the right supramarginal gyrus ($p < 0.05$, corrected; Figure 4(a) and (b)). The dlPFC seeds (left and right) showed weaker connectivity to their contralateral homolog ($p < 0.05$, corrected; Figure 4(c) and (d)). Single-group maps from each seed are shown in Figures S2 to S5. Significant clusters from each analysis are shown in Table S1.

Discussion

In this multimodal study, we report structural and functional network disruptions, as well as associations with symptom severity, in a sample of unmedicated individuals with PTSD. Structural alterations include smaller grey matter volume in the cerebellum (right cerebellar crus) and weaker anatomical covariance between this cerebellum seed and the contralateral middle temporal gyrus in

the PTSD compared to the HC group. Functionally, the PTSD group exhibited weaker whole-brain connectivity in the dlPFC, mPFC and cerebellum. Weaker whole-brain functional connectivity in the cerebellum and smaller grey matter volume in the dlPFC were associated with greater severity of PTSD symptoms. Follow-up seed connectivity indicated weaker connectivity within major nodes of the CEN (left and right dlPFC) in the PTSD sample. Individuals with PTSD also exhibited weaker connectivity between nodes of the DMN (mPFC and cerebellum) and the supramarginal gyrus.

Alterations in the cerebellum were identified in PTSD across modalities, with reductions observed in both grey matter volume and whole-brain functional connectivity. The cerebellum (literally ‘little brain’) has, until recently, been largely ignored in psychiatric disorders, in part due to the traditional conception that the cerebellum’s role is confined to motor function.³⁰ However, convergent findings from neuroimaging and lesion studies have led to a reconceptualization of the cerebellum as playing an important role in cognition and emotion.^{31–33} It is now

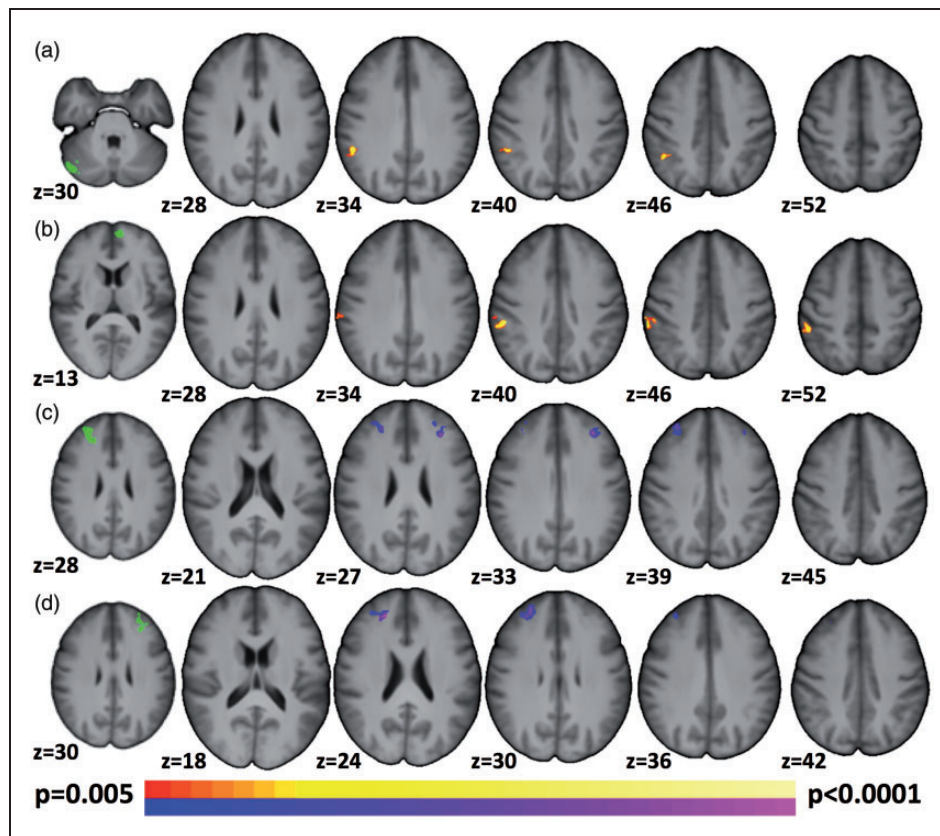


Figure 4. Seed-based connectivity. Seeds are shown in the left column of images (green). (a) Higher connectivity (lower negative connectivity) between cerebellum seed and right supramarginal gyrus ($p < 0.05$, corrected) in PTSD versus HC groups. (b) Greater connectivity (lower negative connectivity) between mPFC seed and right supramarginal gyrus ($p < 0.05$, corrected) in PTSD versus HC groups. (c and d) Lower connectivity between left and right dlPFC and their contralateral homolog ($p < 0.05$, corrected) in PTSD versus HC groups.

known that the cerebellum receives and sends information to non-motor cortical areas, including prefrontal regions responsible for higher cognitive function. Indeed, the majority of the cerebellum maps to cerebral association networks in an organized manner.³³ In addition to identifying structural and functional cerebellar alterations in PTSD, we observed a correlation between functional connectivity in the cerebellum and both overall symptom severity and severity in the four symptom domains specified in the DSM-5 (intrusion symptoms, avoidance, NACM and hyperarousal), suggesting a non-specific role for the cerebellum in PTSD symptomatology. Lesions to the cerebellum can result in anxiety, aggression, irritability and distractibility,³⁴ symptoms that are relevant to PTSD. In line with our findings, structural and functional cerebellar abnormalities in PTSD have been reported previously. For example, cerebellar volume has been shown to be lower in adolescents³⁵ and adults with PTSD,^{36,37} with cerebellum volume negatively correlating with PTSD symptoms. Furthermore, meta-analyses of both resting-state³⁸ and task-based³⁹ neuroimaging studies indicate hypoactive cerebellar function in PTSD. A recent study found alterations in functional connectivity from distinct cerebellar seeds to brain regions involved in emotional regulation, somatosensory processing and memory retrieval in PTSD, with distinct patterns of cerebellar alterations in the dissociative subtype of PTSD.⁴⁰ Our findings, therefore, add to a growing body of evidence implicating a role for the cerebellum in the pathophysiology of PTSD and highlight the gaps that continue to exist in our understanding of brain structure and function in this disorder.

Dysregulation in dlPFC ICD connectivity is consistent with previous work implicating dlPFC abnormalities in PTSD.¹⁴ Lower dlPFC connectivity has been previously observed in PTSD,⁴¹ and task-based studies have consistently shown dlPFC hypoactivation in PTSD.¹⁴ The dlPFC subserves higher order cognitive functions such as working memory and attentional control and is a major hub of the CEN.⁴² It also has multiple reciprocal connections to limbic structures such as the amygdala and hippocampus.⁴³ Aberrant dlPFC function may, therefore, be associated with reduced inhibitory control over limbic structures such as the amygdala, which is consistently shown to be altered in PTSD.¹ Indeed, meta-analyses indicate that impaired functional relationships between PFC and limbic regions are linked to emotional dysregulation⁴⁴ and, specifically, to PTSD.^{14,45} dlPFC is also a target for repetitive transcranial magnetic stimulation (rTMS) for the treatment of PTSD symptomatology, with a meta-analysis indicating that increasing cortical excitability in the dlPFC through active rTMS was associated with a significant reduction in PTSD symptoms.⁴⁶ The fact that we found correlations between lower dlPFC grey matter volume and greater severity of

PTSD symptoms provides further support for dlPFC dysregulation in PTSD and suggests that targeting normalization of dlPFC structure and function may help to alleviate PTSD symptoms.

ICD connectivity was also lower in the mPFC, a core component of the DMN, in PTSD compared to HC individuals. This is consistent with three meta-analyses of resting-state neuroimaging studies identifying mPFC hypoactivity in PTSD compared to HC individuals.^{14,47,48} In conjunction with reduced mPFC functioning, meta-analyses have confirmed hyperactivity in the amygdala in PTSD.^{14,48} Such a pattern is understood to reflect a lack of regulatory control over emotion in PTSD, and the mPFC is thus considered to play a critical role in the pathophysiology of PTSD. Reduced mPFC function in PTSD has been linked to disturbances within the DMN,^{5,6} which is associated with internally focused thought, autobiographical memory and mind-wandering, and whose activity is typically increased in the absence of a cognitively-demanding task.⁴⁹ Our study, therefore, adds to the growing literature suggesting weakened functional integration in the DMN at rest in those with PTSD. A weakened DMN could be associated with disrupted self-referential processing, which can lead to dissociative symptoms and impairments in autobiographical memory, both of which have been implicated in PTSD.⁵⁰

Our seed-based findings point to disruptions in intrinsic connectivity networks in PTSD, specifically in the CEN and the DMN. Weaker seed-based connectivity between left and right dlPFC seeds and their contralateral homologs suggests less integration within the CEN (the dlPFC being a core hub of the CEN). Less integration within the CEN may account for cognitive disturbances in PTSD⁵¹ and be related to reduced top-down control over limbic structures and resultant emotional dysregulation.⁴⁴ The reduced ICD connectivity in mPFC and in the cerebellum, a peripheral component of the DMN,^{52–54} adds to the growing literature implicating dysfunction of the DMN in PTSD.^{5–8} Furthermore, using the cerebellum seed identified in the TBM analysis, we observed reduced anatomical covariance with the middle temporal gyrus, also part of the DMN,⁴⁹ in PTSD versus HC groups. This raises the possibility of a structure–function relationship between nodes of the DMN in PTSD, which could be associated with the clinical presentation of disturbances in self-referential processing and autobiographical memory observed in PTSD.⁵⁰

At rest, the default-mode and ‘task-positive’ networks (such as the CEN) are typically strongly negatively correlated.⁴² These cross-network anticorrelations reflect competing functions. For example, the typically observed anticorrelation between the DMN and the CEN at rest is thought to reflect opposing functions; that is, internal awareness and self-referential processing in the case of the DMN, and external monitoring and focused attention

in the case of the CEN.⁴² The connectivity patterns identified from the seed-based analysis show less of an ‘anti-correlation’ between nodes of the CEN and the DMN. Specifically, both cerebellum and mPFC seeds exhibited increased connectivity (i.e., reduced negative correlation) with the supramarginal gyrus, a component of the CEN.⁵⁵ This anticorrelation between nodes of the DMN and the CEN suggests a possible ‘blurring’ of these typically opposed networks in PTSD. This blurring could be associated with difficulties in switching between internal and external worlds, possibly reflecting an impaired ability to distinguish internal from external threat-related cues. Specific to PTSD, conditioned responses of fear to external stimuli are generalized not only to a range of external cues but also to internal cues including thoughts and mental imagery, which might be subserved by disturbances in the DMN and CEN. In line with this,⁷ we found a positive correlation between frequency of dissociative experiences and connectivity between nodes of the DMN and the dlPFC, further implicating alterations in the relation between the DMN and the CEN in PTSD.

There are several limitations to this study. First, our sample size was modest; however, we were still able to detect group differences, as well as correlations with PTSD symptomatology, with current best practices for multiple comparison correction. Second, the HC group was not matched for trauma exposure. A comparison of trauma-exposed individuals with and without PTSD would be the most informative in elucidating the mechanisms underlying development of, and resilience to, PTSD. Third, there was a scanner upgrade half way through the study. However, the proportion of PTSD and HC subjects was equal before and after the upgrade. Between-group functional and structural region of interest (ROI) values were examined independently for each scanner and findings remained significant. This is in line with our previous work indicating that ICD values are stable across scanner types.⁵⁶

Fourth, 16 of the 21 PTSD individuals had comorbid MDD, which aligns with the high comorbidity and symptomatic overlap between PTSD and depressive symptoms.⁵⁷ A larger multimodal investigation into PTSD with and without comorbid MDD is necessary to tease apart any network-level differences between these two groups. We found significant correlations between functional/structural measures and PTSD symptoms, but no correlations with MDD symptoms, suggesting that the observed network disturbances in our sample may be driven by PTSD as opposed to MDD symptomatology. In our previous study in MDD using similar methodology,⁵⁸ we observed connectivity and covariance patterns distinct from the current findings in PTSD. Previous activation and seed-based connectivity studies in PTSD have shown, in addition to the PFC abnormalities, alterations in amygdala, hippocampus and insula

PTSD.¹ Different findings between previous work and the current study can be attributed to methodological differences such as using seed-based versus data-driven approaches, differences in multiple comparison correction and performing global signal regression or to differences in patient samples.

Conclusion

This multimodal study shows overlapping structural and functional alterations in PTSD and associations with symptom severity. Findings converge on regions of the PFC and the cerebellum, and seed-based results point to alterations within and between the default mode and the CENs. Cerebellar and PFC pathologies co-occur across psychiatric diagnoses such as autism and schizophrenia,⁵⁹ and neuroanatomical evidence has demonstrated closed-loop connectivity between the cerebellum and the PFC.⁵² Whether the observed abnormalities in the cerebellum and PFC are related in PTSD requires further investigation. While the pattern and extent of whole-brain network changes in PTSD needs further confirmation, we add to the evidence indicating that PTSD is a system-level disorder that affects multiple brain networks at the functional and the structural levels. Identifying treatments that target network alterations in PTSD may lead to the development of more effective treatments for this disorder. Furthermore, our findings add to the mounting evidence implicating a key role for the cerebellum in PTSD and underscore the importance of considering the cerebellum in pathophysiological models of PTSD.

Acknowledgments

The authors thank the staff at Yale’s Magnetic Resonance research Center, the National Center for PTSD (West Haven Campus), the Yale Center for Clinical investigation, and the individuals who took part in the study.

Declaration of Conflicting Interests

The author(s) declared the following potential conflicts of interest with respect to the research, authorship, and/or publication of this article: Dr. Krystal acknowledges the following relevant financial interests. He is a cosponsor of a patent for the intranasal administration of ketamine for the treatment of depression that was licensed by Janssen Pharmaceuticals, the maker of s-ketamine. He has a patent related to the use of riluzole to treat anxiety disorders that was licensed by Biohaven Medical Sciences. He has stock or stock options in Biohaven Medical Sciences, ARet Pharmaceuticals, Blackthorn Therapeutics, and Luc Therapeutics. He consults broadly to the pharmaceutical industry, but his annual income over the past year did not exceed \$5000 for any organization. He receives over \$5000 in income from the Society of Biological Psychiatry for editing the journal *Biological Psychiatry*. He has fiduciary responsibility for the International College of Neuropsychopharmacology as

president of this organization. The other authors declare no conflict of interest.

Funding

The author(s) disclosed receipt of the following financial support for the research, authorship, and/or publication of this article: Funding was provided by the VA National Center for PTSD (Esterlis, Krystal, Pietrzak), NIMH Grants K01MH092681 and R01MH104459 (Esterlis), the Dana Foundation (Esterlis), the Nancy Taylor Foundation (Esterlis), and the Yale Center for Clinical Investigation.

References

- Liberzon I, Sripada CS. The functional neuroanatomy of PTSD: a critical review. *Prog Brain Res* 2008; 167: 151–169.
- Karl A, Schaefer M, Malta LS, Dörfel D, Rohleder N, Werner A. A meta-analysis of structural brain abnormalities in PTSD. *Neurosci Biobehav Rev* 2006; 30: 1004–1031.
- Craddock RC, Jabdi S, Yan C-G, et al. Imaging human connectomes at the macroscale. *Nat Methods* 2013; 10: 524–539.
- Evans AC. Networks of anatomical covariance. *Neuroimage* 2013; 80: 489–504.
- DiGangi JA, Tadayyon A, Fitzgerald DA, et al. Reduced default mode network connectivity following combat trauma. *Neurosci Lett* 2016; 615: 37–43.
- Lanius R, Bluhm R, Coupland N, et al. Default mode network connectivity as a predictor of post-traumatic stress disorder symptom severity in acutely traumatized subjects. *Acta Psychiatr Scand* 2010; 121: 33–40.
- Bluhm RL, Williamson PC, Osuch EA, et al. Alterations in default network connectivity in posttraumatic stress disorder related to early-life trauma. *J Psychiatr Neurosci* 2009; 34: 187–194.
- Sripada RK, King AP, Welsh RC, et al. Neural dysregulation in posttraumatic stress disorder: evidence for disrupted equilibrium between salience and default mode brain networks. *Psychosom Med* 2012; 4: 904–911.
- Daniels JK, McFarlane AC, Bluhm RL, et al. Switching between executive and default mode networks in posttraumatic stress disorder: alterations in functional connectivity. *J Psychiatry Neurosci* 2010; 35: 258–266.
- Birn RM, Patriat R, Phillips ML, Germain A, Herringa RJ. Childhood maltreatment and combat posttraumatic stress differentially predict fear-related fronto-subcortical connectivity. *Depress Anxiety* 2014; 31: 880–892.
- Jacques PLS, Kragel PA, Rubin DC. Neural networks supporting autobiographical memory retrieval in posttraumatic stress disorder. *Cogn Affect Behav Neurosci* 2013; 13: 554–566.
- Cisler JM, Steele JS, Smitherman S, Lenow JK, Kilts CD. Neural processing correlates of assaultive violence exposure and PTSD symptoms during implicit threat processing: a network-level analysis among adolescent girls. *Psychiatry Res* 2013; 214: 238–246.
- Yehuda R, Hoge CW, McFarlane AC, et al. Post-traumatic stress disorder. *Nat Rev Dis Primers* 2015; 1: 15057.
- Patel R, Spreng RN, Shin LM, Girard TA. Neurocircuitry models of posttraumatic stress disorder and beyond: a meta-analysis of functional neuroimaging studies. *Neurosci Biobehav Rev* 2012; 36: 2130–2142.
- Jin C, Qi R, Yin Y, et al. Abnormalities in whole-brain functional connectivity observed in treatment-naive post-traumatic stress disorder patients following an earthquake. *Psychol Med* 2014; 44: 1927–1936.
- Zhang Y, Xie B, Chen H, Li M, Liu F, Chen H. Abnormal functional connectivity density in post-traumatic stress disorder. *Brain Topogr* 2016; 29: 405–411.
- Abdallah CG, Wrocklage KM, Averill CL, et al. Anterior hippocampal dysconnectivity in posttraumatic stress disorder: a dimensional and multimodal approach. *Transl Psychiatry* 2017; 7: e1045.
- Hua X, Leow AD, Lee S, Klunder AD, Toga AW, Lepore N, et al. 3D characterization of brain atrophy in Alzheimer's disease and mild cognitive impairment using tensor-based morphometry. *Neuroimage* 2008; 41: 19–34.
- Scheinost D, Benjamin J, Lacadie C, et al. The intrinsic connectivity distribution: a novel contrast measure reflecting voxel level functional connectivity. *Neuroimage* 2012; 62: 1510–1519.
- Scheinost D, Holmes SE, DellaGioia N, et al. Multimodal investigation of network level effects using intrinsic functional connectivity, anatomical covariance, and structure-to-function correlations in unmedicated major depressive disorder. *Neuropsychopharmacology* 2018; 43: 1119–1127.
- American Psychiatric Association. *Diagnostic and Statistical Manual of Mental Disorders*, 5th ed. Washington, DC: American Psychiatric Association, 2013.
- First MB, Spitzer RL, Gibbon M, Williams JB. *User's Guide for the Structured Clinical Interview for DSM-IV Axis I Disorders SCID-I: Clinician Version*. Washington, DC: American Psychiatric Association, 1997.
- Montgomery SA, Asberg M. A new depression scale designed to be sensitive to change. *Br J Psychiatry* 1979; 134: 382–389.
- Hamilton M. Rating depressive patients. *J Clin Psychiatry* 1980; 41: 21–24.
- Hamilton M. Development of a rating scale for primary depressive illness. *Br J Soc Clin Psychol* 1967; 6: 278–296.
- Beck AT, Steer RA. Internal consistencies of the original and revised Beck Depression Inventory. *J Clin Psychol* 1984; 40: 1365–1367.
- Joshi A, Scheinost D, Okuda H, et al. Unified framework for development, deployment and robust testing of neuroimaging algorithms. *Neuroinformatics* 2011; 9: 69–84.
- Scheinost D, Kwon SH, Lacadie C, et al. Alterations in anatomical covariance in the prematurely born. *Cereb Cortex* 2017; 27: 534–543.
- Scheinost D, Papademetris X, Constable RT. The impact of image smoothness on intrinsic functional connectivity and head motion confounds. *Neuroimage* 2014; 95: 13–21.
- Lee HW, Arora J, Papademetris X, et al. Altered functional connectivity in seizure onset zones revealed by fMRI intrinsic connectivity. *Neurology*. 2014; 83: 2269–2277.
- Botez Cerebellum MI, Ramachandran VS. (Ed.), *Encyclopedia of Human Behavior*, New York: Academic Press, 1999: p. 2002.
- Schmahmann JD, Caplan D. Cognition, emotion and the cerebellum. *Brain* 2006; 129: 290–292.

33. Schutter DJ, Van Honk J. The cerebellum on the rise in human emotion. *Cerebellum* 2005; 4: 290–294.
34. Buckner RL. The cerebellum and cognitive function: 25 years of insight from anatomy and neuroimaging. *Neuron* 2013; 80: 807–815.
35. Schmahmann JD, Weilburg JB, Sherman JC. The neuropsychiatry of the cerebellum—insights from the clinic. *Cerebellum*. 2007; 6: 254–267.
36. De Bellis MD, Kuchibhatla M. Cerebellar volumes in pediatric maltreatment-related posttraumatic stress disorder. *Biol Psychiatry* 2006; 60: 697–703.
37. Baldaçara L, Jackowski AP, Schoedl A, et al. Reduced cerebellar left hemisphere and vermal volume in adults with PTSD from a community sample. *J Psychiatr Res* 2011; 45: 1627–1633.
38. Baldaçara L, Borgio JGF, Araújo C, et al. Relationship between structural abnormalities in the cerebellum and dementia, posttraumatic stress disorder and bipolar disorder. *Dement Neuropsychol* 2012; 6: 203–211.
39. Koch SBJ, van Zuiden M, Nawijn L, Frijling JL, Veltman DJ, Olff M. Aberrant resting-state brain activity in posttraumatic stress disorder: a meta-analysis and systematic review. *Depress Anxiety* 2016; 33: 592–605.
40. Hayes JP, Hayes SM, Mikedis AM. Quantitative meta-analysis of neural activity in posttraumatic stress disorder. *Biol Mood Anxiety Disord* 2012; 2: 9.
41. Rabellino D, Densmore M, Théberge J, McKinnon MC, Lanius RA. The cerebellum after trauma: resting-state functional connectivity of the cerebellum in posttraumatic stress disorder and its dissociative subtype [published online ahead of print April 17, 2018]. *Hum Brain Mapp*. <https://doi.org/10.1002/hbm.24081>. doi:10.1002/hbm.24081.
42. Reuveni I, Bonne O, Giesser R, et al. Anatomical and functional connectivity in the default mode network of posttraumatic stress disorder patients after civilian and military-related trauma. *Hum Brain Mapp* 2016; 37: 589–599.
43. Fox MD, Snyder AZ, Vincent JL, Corbetta M, Van Essen DC, Raichle ME. The human brain is intrinsically organized into dynamic, anticorrelated functional networks. *Proc Natl Acad Sci U S A*. 2005; 102: 9673–9678.
44. Hartley CA, Phelps EA. Changing fear: the neurocircuitry of emotion regulation. *Neuropsychopharmacology* 2010; 35: 136–146.
45. Kober H, Barrett LF, Joseph J, Bliss-Moreau E, Lindquist K, Wager TD. Functional grouping and cortical-subcortical interactions in emotion: a meta-analysis of neuroimaging studies. *Neuroimage* 2008; 42: 998–1031.
46. Etkin A, Wager TD. Functional neuroimaging of anxiety: a meta-analysis of emotional processing in PTSD, social anxiety disorder, and specific phobia. *Am J Psychiatry* 2007; 164: 1476–1488.
47. Berlim MT, Van den Eynde F. Repetitive transcranial magnetic stimulation over the dorsolateral prefrontal cortex for treating posttraumatic stress disorder: an exploratory meta-analysis of randomized, double-blind and sham-controlled trials. *Can J Psychiatry* 2014; 59: 487–496.
48. Wang T, Liu J, Zhang J, et al. Altered resting-state functional activity in posttraumatic stress disorder: a quantitative meta-analysis. *Sci Rep* 2016; 6: 27131.
49. Etkin A, Wager TD. Functional neuroimaging of anxiety: a meta-analysis of emotional processing in PTSD, social anxiety disorder, and specific phobia. *Am J Psychiatry* 2007; 164: 1476–1488.
50. Buckner RL, Andrews-Hanna JR, Schacter DL. The brain's default network. *Ann N Y Acad Sci* 2008; 1124: 1–38.
51. Lanius RA, Vermetten E, Loewenstein RJ, et al. Emotion modulation in PTSD: clinical and neurobiological evidence for a dissociative subtype. *Am J Psychiatry* 2010; 167: 640–647.
52. Hayes JP, VanElzakker MB, Shin LM. Emotion and cognition interactions in PTSD: a review of neurocognitive and neuroimaging studies. *Front Integr Neurosci* 2012; 6: 89.
53. Buckner RL, Krienen FM, Castellanos A, Diaz JC, Yeo BT. The organization of the human cerebellum estimated by intrinsic functional connectivity. *J Neurophysiol* 2011; 106: 2322–2345.
54. Habas C, Kamdar N, Nguyen D, et al. Distinct cerebellar contributions to intrinsic connectivity networks. *J Neurosci* 2009; 29: 8586–8594.
55. Fransson P. How default is the default mode of brain function? Further evidence from intrinsic BOLD signal fluctuations. *Neuropsychologia* 2006; 44: 2836–2845.
56. Yeo BT, Krienen FM, Sepulcre J, et al. The organization of the human cerebral cortex estimated by intrinsic functional connectivity. *J Neurophysiol* 2011; 106: 1125–1165.
57. Noble S, Scheinost D, Finn ES, et al. Multisite reliability of MR-based functional connectivity. *Neuroimage* 2017; 146: 959–970.
58. Gros DF, Price M, Magruder KM, Frueh BC. Symptom overlap in posttraumatic stress disorder and major depression. *Psychiatry Res* 2012; 196: 267–270.
59. Scheinost D, Holmes SE, DellaGioia N, et al. Multimodal investigation of network level effects using intrinsic functional connectivity, anatomical covariance, and structure-to-function correlations in unmedicated major depressive disorder. *Neuropsychopharmacology* 2018; 43: 1119–1127.
60. Mittleman GUY, Goldowitz D, Heck DH, Blaha CD. Cerebellar modulation of frontal cortex dopamine efflux in mice: relevance to autism and schizophrenia. *Synapse* 2008; 62: 544–550.